Improved PV Performance Modelling by Combining the PV_LIB Toolbox with the Loss Factors Model (LFM)

Juergen Sutterlueti[1], Steve Ransome[2], Joshua Stein[3] and Joerg Scholz[1]

[1] Gantner Instruments Environment Solutions GmbH, 08297 Zwoenitz/ Germany
[2] Steve Ransome Consulting Ltd, KT2 6AF #99, Kingston upon Thames, UK
[3] Sandia National Laboratories, P.O. Box 5800 MS 1033, Albuquerque, NM 87185 USA.

Abstract — PV project investments need comprehensive plant monitoring data in order to validate performance and to fulfil expectations. Algorithms from PV-LIB and Loss Factors Model are being combined to quantify their prediction improvements at Gantner Instruments' Outdoor Test facility at Tempe AZ on multiple Tier 1 technologies. The validation of measured vs. predicted long term performance will be demonstrated to quantify the potential of IV scan monitoring. This will give recommendations on what parameters and methods should be used by investors, test labs, and module producers.

***Index Terms* — Energy, Meteorology, Modeling, Photovoltaic systems, Power, Simulation.**

I. INTRODUCTION

PV project investments require continuous, accurate and traceable plant monitoring data in order to determine the actual vs. design performance and to fulfil owner/investor expectations.

Algorithms from the "PV Performance Modeling Collaborative" (PVPMC) and "Loss Factors Model" (LFM) are being combined to test out their prediction improvements at Gantner Instruments' (GI) Outdoor Test facility at Tempe AZ on multiple Tier 1 technologies including c-Si, CdTe and CIGS.

The PV_LIB Toolbox was originally developed at Sandia National Laboratories and has been expanded by contributions from members of the PVPMC [1]. A standard library of PV algorithms includes solar position, irradiance translation, module temperature, and array and inverter performance. PV_LIB is available in MatLab and Python versions [2] [3].

The LFM has been developed and is being used by SRCL and Gantner Instruments to produce optimum PV performance simulation accuracy with determination of performance coefficients, quantification of any instability and fault finding diagnosis [4] [5].

The validation and comparisons of the measured vs. predicted (long term) performance will be demonstrated in this paper to quantify the potential benefits of continuous IV scan monitoring. We will provide recommendations on what parameters and methods should be used by investors, test labs, and module producers. Validated functions are available in the gantner.webportal for advanced utility scale analysis and prediction. Providing more accurate performance analysis, indication of abnormal loss or trends leads to more effective O&M and risk reduction for owners.

II. OUTDOOR MEASUREMENTS

Gantner Instruments' Outdoor Test facility (OTF) in Tempe, AZ (figure 1) measures IV curves every minute for 24 fixed modules and 6 on a 2D tracker [6]. It has been running since July 2010 with a 98% uptime.

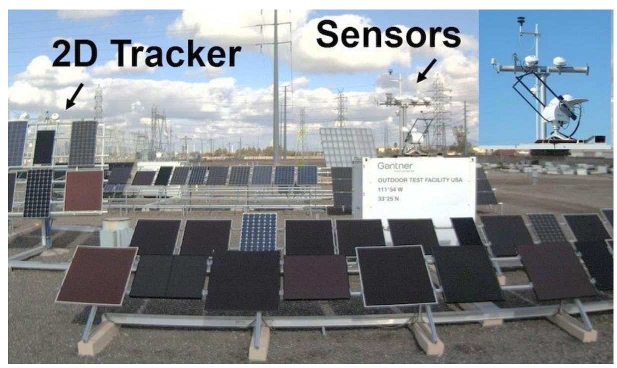

Fig 1. Gantner Instruments OTF in Tempe, Arizona.

Table I lists some of the GI OTF meteorological measurements.

TABLE I. GI OTF MEASUREMENTS

Name	Description	Units
G_H	Global Horizontal Irradiance	kW/m²
D_H	Diffuse Horizontal Irradiance	kW/m²
B_N	Beam Normal Irradiance	kW/m²
G_I	Global Inclined Irradiance (Pyranometers and c-Si ref cells)	kW/m²
T_{AMB}	Ambient Temperature	C
T_{MOD}	Back of Module Temperatures	C
WS	Wind Speed	ms^{-1}
WD	Wind Direction	°
RH	Relative Humidity	%
G(λ)	Spectral Irradiance G(350– 1050nm)	W/m²/nm

III. VALIDATING PV_LIB AND LFM ALGORITHMS

Using synchronized, 1 minute measured data from a year at the Tempe Site (which is defined by its latitude and longitude; array tilt and azimuth) calculations were made with the PV_LIB routines and checked with existing site calculations (e.g. solar position), actual meteorological measurements (irradiance, temperature, spectrum etc.) and measured PV performance as below (*A to F*).

A. "GI calculated" vs. PV_LIB Solar Position

The PV_LIB solar elevation and azimuth (calculated using the *pvl_spa* function) were compared with the predictions from the GI site, which used a less sophisticated algorithm (SUNAE) to calculate sun position. Differences are shown in figure 2. Both azimuth and elevation are mostly within ±2°. These differences are typical, since the *pvl_spa* model is based on NREL's Sun Position Algorithm [7] which includes details not addressed by simpler models (e.g., refraction, nutation, etc.).

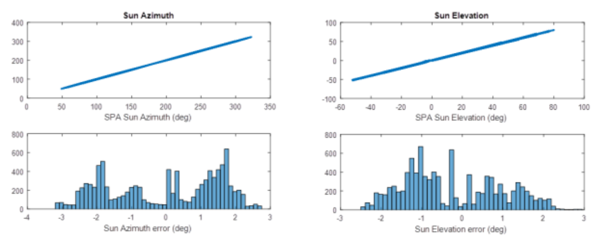

Fig 2. Comparing PV_LIB calculations of solar elevation and azimuth with the internal data from GI

B. Predicted Tilted irradiance from diffuse Sky model

PV_LIB contains several methods for estimating tilted global G_I, as a function of diffuse horizontal D_H and beam normal B_N (with angle of incidence). Figure 3 shows the correlation between six anisotropic or isotropic sky models calculated vs. measured G_I. The Perez model is the best with low bias and random errors; the Klucher and King models are nearly as good.

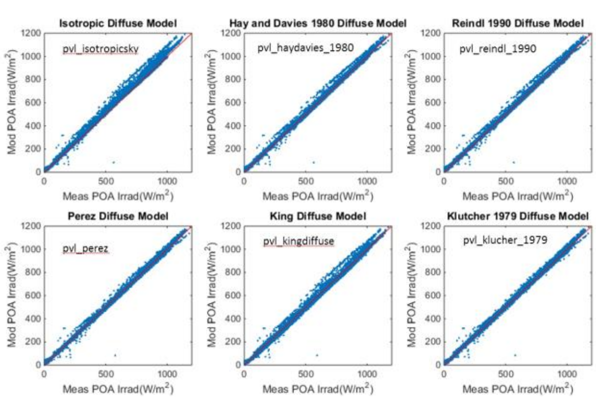

Fig 3. Comparing calculated vs. measured tilted plane irradiance from six PV_LIB anisotropic or isotropic diffuse sky models (*pvl_isotropicsky, pvl_haydavies_1980, pvl_reindl_1990, pvl_perez, pvl_kingdiffuse, and pvl_klucher_1979*).

C. Spectral content vs. solar altitude and azimuth

Blue Fraction is defined as "blue light"/"c-Si absorbable light" (1) and is an alternative to the average photon energy (APE) which depends on the lower and upper limits of measured wavelength.

$$\text{Blue Fraction} = \frac{\sum G_{350-650\,\text{nm}}}{\sum G_{350-1050\,\text{nm}}} \tag{1}$$

For AM1.5 the Blue Fraction ~0.52, a higher number comes from a bluer spectrum, a lower value means redder than AM1.5.

At most sites the solar spectrum is not measured but if needed is inferred from solar elevation angles. This may work well under clear sky conditions but not so well under cloudy skies where the clouds absorb more red light than blue. GI use the Blue Fraction as a "rule of thumb" to roughly quantify spectral irradiance.

Figure 4 gives the measured Blue Fraction (y axis) vs. Air Mass (derived just from the solar height - x axis) for different clearness indices (kTh) from 0.2 (mostly obscured) to 1.0 (clear) at the GI Tempe site. Clear skies usually have a kTh~0.8 (meaning 80% of the extraterrestrial horizontal irradiance reaches the ground, the other 20% is absorbed or reflected by the atmosphere). This is shown in pale green with linear fits from AM1 to AM6. The value at AM1.5 is around 52% and it falls around 2% for each "integer AM" increase. Other clearness indexes follow a similar trend with the overall shift being towards blue rich when the clearness falls.

.

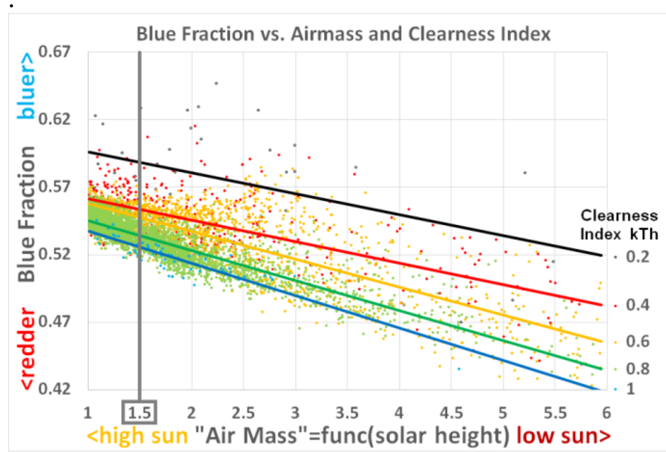

Fig 4. Measured Blue Fraction vs. Air Mass (Solar height) for different clearness indices at the GI site at Tempe.

Figure 5 plots the average measured blue fraction vs. solar altitude and azimuth for 1 minute data at the GI Tempe facility (which has predominantly clear skies).

A Blue Fraction of 0.52~AM1.5 is shown in yellow with other colours indicating bluer or redder spectra. In general the higher the solar altitude then the bluer the spectrum and vice versa – also a little bluer (clearer) in the morning than the afternoon. There are two spots of “very blue rich light >0.59” at low solar altitude and azimuths of <80 ENE ❶ and >280 WNW ❷ when the sun is behind the module so there’s no direct light, only diffuse and hence a bluer than expected spectrum.

There is also a localized spot of blue rich light at 100° azimuth and 10° solar altitude ❸ which we will identify in the next section *D.*

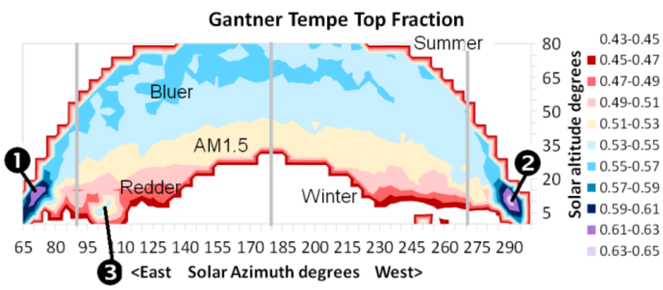

Fig 5. Average measured Blue Fraction vs. solar altitude and solar azimuth for GI’s Tempe facility

D. Isc vs Angle of Incidence and shading

Figure 6 plots the normalized I_{SC} (2) for a standard c-Si screen print module vs. solar altitude and azimuth at GI Tempe.

$$nI_{SC} = \frac{I_{SC.MEASURED}}{I_{SC.STC} * GI_{cSI.REFCELL}} \qquad (2)$$

nI_{SC} is smooth over most of the solar positions, becoming a little higher for large azimuths away from south <90 ENE ❷ and >270 WNW ❶ (presumably the ARC on the c-Si module gives better off axis reflectivity than the reference cell). However at point ❸ (as in figure 3) the current drops 20-30% suggesting it was due to shading. This would filter out some of the red direct light from the low sun making the resultant spectrum go bluer as seen in figure 3.

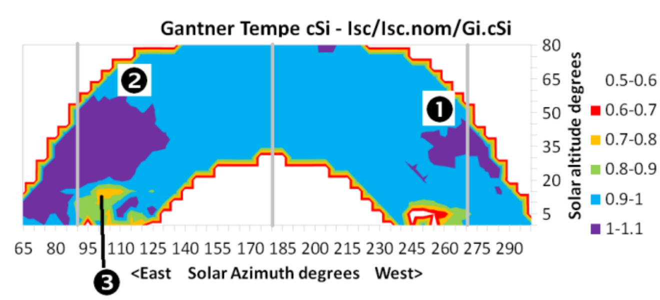

Fig 6. Average normalized I_{SC} vs. solar altitude and solar azimuth for a typical c-Si module at GI’s Tempe facility

E. Module Temperature rise above ambient vs. wind speed (and irradiance)

Module and cell temperatures rise above ambient depending on plane of array irradiance, wind speed, the manufacturing technology (e.g. glass-glass, glass-polymer etc.) and also the mounting method (e.g. freely ventilated back, insulated back, bipv etc.) [8]. The relevant PV_LIB function is

```
pvl_sapmcelltemp(E=Irradiance, Wspd, Tamb, modelt)
```

There are three empirical coefficients dependent on the technology and mounting method. Recommended values can be found on the PVPMC website.

Figure 7 plots the modelled vs. measured average temperature rise above ambient vs. wind speed (x axis) and irradiance (plots) for a free back CdTe module at GI’s Tempe site using the default PV_LIB coefficients. A good overall agreement can be seen with discrepancies generally <±2C. (The empirical coefficients could be further optimized to give a better fit for yield prediction.)

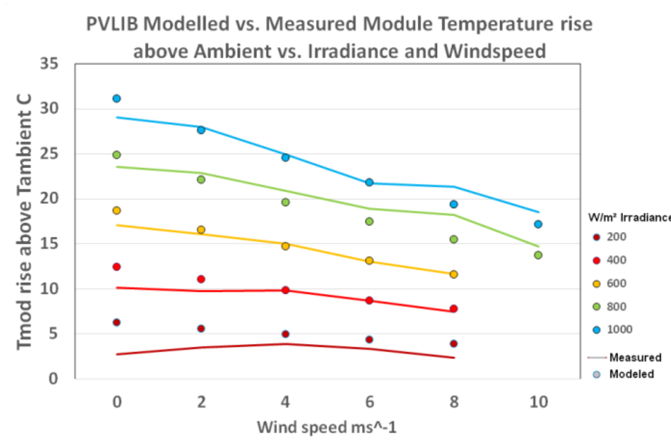

Fig 7. PV_LIB modelled vs. average measured module temperature rise above T_{AMB} for a CdTe module at GI Tempe against wind speed (x axis) and irradiance (lines).

F. Sensor angle of incidence

Pyranometers tend to have a slightly better angular acceptance response than c-Si reference cells as their domes reflect less light away than a flat plate panel even with antireflective coating. Figure 8 shows the results of comparing the irradiance reported by a plane of array pyranometer versus a plane of array crystalline reference cell vs. horizontal beam fraction and angle of incidence for GI’s Tempe site. This can be used to perform angle-of-incidence (AOI) corrections for flat plate panels with only pyranometer sensors – when c-Si reference cells are used then the angular correction needed is small. Beam fractions are usually between 0.2 (mostly diffuse) and 0.8 (mostly direct), at the GI Tempe site the angle of incidence only gets below 10° for a short time (spring/autumn equinox at solar noon) also data above 80° AOI has a lot of scatter so the graph does not include some extreme values for clarity. Nevertheless the $G_{c\text{-}Si}/G_{PYR}$ approaches 100% for angle of incidence <10° at any beam fraction (as expected from calibrated sensors but note there's no spectral correction) and falls off as the angle of incidence increases, slightly faster under direct than diffuse conditions. As a rule of thumb the graph suggests a value of about 85% at an AOI of 65° and BF=0.5 meaning the c-Si sensor would predict a 15% better low light coefficient than the pyranometer would suggest under these conditions

.

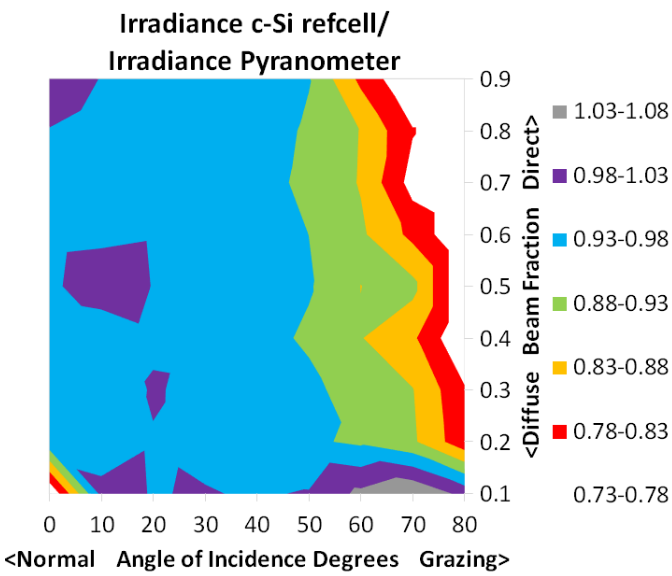

Fig 8. Average irradiance measured by the POA c-Si reference cell divided by that from a POA pyranometer measured at GI Tempe. No spectral corrections are done.

IV. The Loss Factors Model

The LFM fits IV curves very well under normal weather conditions [4].

The PV current depends on the following parameters in table II showing the modelled dependence on whether a c-Si reference cell is used or a Pyranometer.

TABLE II. LFM Parameters Affecting I_{SC}, I_{MP}

	Parameter	c-Si Reference Cell	Pyranometer
1	Shading	Similar near shading if close	Similar near shading if close
2	Spectrum	Similar if c-Si module	Will be different
3	Angle of incidence	Similar if same manufacture	Will be different
4	Soiling	May be similar if coplanar	Different if Glass dome
5	Snow	May be similar if coplanar	Different if Glass dome
6	Temperature	Small effect	Small effect

Previously LFM values have been derived by normalizing measurements with a c-Si reference sensor. Fits have been done to "good conditions" i.e. reasonable high irradiance, near noon (so low angle of incidence), unshaded and non-snow covered conditions. Extreme conditions for parameter fitting have been removed by filtering on limits (such as 'AOI<60 degrees' or 'sun height >15') to get rid of the "scattered" points that may be hard to fit but filtering gets rid of some good points too. For example if there is a building shading 15 degrees high to the east but a low horizon to the west, filtering 'sun height>15' removes some otherwise good low solar height measurements in the west.

PV Voltages depend on the parameters in table III.

TABLE III. LFM Parameters Affecting V_{OC}, V_{MP}

	Parameter	Comments
1	Cell Temperature	Estimate from Ambient and Cell Back
2	Irradiance	Will be affected by previous ~15 minutes weather (thermal capacity)
3	Wind speed	Will be affected by previous ~15 minutes weather (thermal capacity)
4	Manufacture	e.g. affects thermal capacity
5	Mounting	e.g. how close to roof

The PV_LIB functions already contain PV models (including the 1-diode and SAPM) but in this work the LFM is included to improve the modelling accuracy [5]. An outcome of this work will be to add the LFM to the PV_LIB Toolbox, allowing greater access.

The LFM is illustrated in figure 9 [4]. It analyses IV curves at different outdoor conditions (irradiance, module temperature, spectrum, angle of incidence etc.) to give six normalized orthogonal parameters (as in Table IV) that characterize a module's performance and can identify the cause and any rate of change of limiting parameters. The product of these 6 parameters gives the normalized efficiency (also known as the DC performance ratio PR_{DC}).

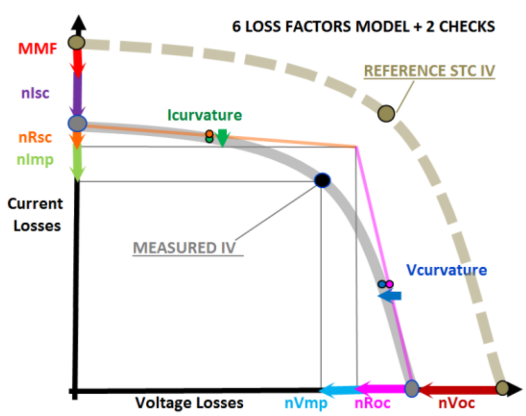

Fig 9. Simplified SRCL/Gantner Instruments Loss Factors Model

TABLE IV. NORMALIZED LFM PARAMETERS

LFM	Performance determining factors include
nI_{SC}	Spectral mismatch, dirt, snow, beam reflectivity vs. AOI
nR_{SC}	$R_{SHUNT}(G_I)$
nI_{MP}	$I_{MP}(G_I)$ corrected for R_{SC}
nV_{MP}	$V_{MP}(G_I)$ corrected for R_{OC}
nR_{OC}	G_I^2 * $R_{SERIES}(G_I)$
nV_{OC}	$V_{OC}(G_I) \sim \ln(G_I/I_O)$, T_{MODULE}
PR_{DC}	= (nI_{SC}*nR_{SC}*nI_{MP}) * (nV_{MP}*nR_{OC}*nV_{OC})

A. PV Performance vs. Irradiance and Temperature

PV module performance is measured over a period of time at differing meteorological conditions such as irradiance, ambient temperature, angle of incidence and spectrum. The 6 LFM parameters are then characterized by fitting as functions of irradiance and temperature. On line checks of performance can be undertaken by comparing measured with data predicted from the earlier test method.

V. IMPROVEMENTS TO LFM FITS USING EMPIRICAL MODELS OF TOP FRACTION, AOI (AND T_{MODULE})

Figure 10 shows predicted vs. measured performance of a CdTe module (top) and a c-Si module (bottom) at Tempe for ~750 random data points. For well-behaved modules the five LFM parameters (except nI_{SC}) can usually be fitted to <±1% accuracy shown as the grey horizontal lines (i.e. the coloured dots are usually within the grey lines for a good fit).

The fit for nI_{SC} is also affected by soiling, snow, angle of incidence reflectivity and spectral response.

It is important to know the T_{MODULE} for the nV_{OC} coefficient. If this is not known then it can be calculated from the PV_LIB ***pvl_sapmcelltemp***

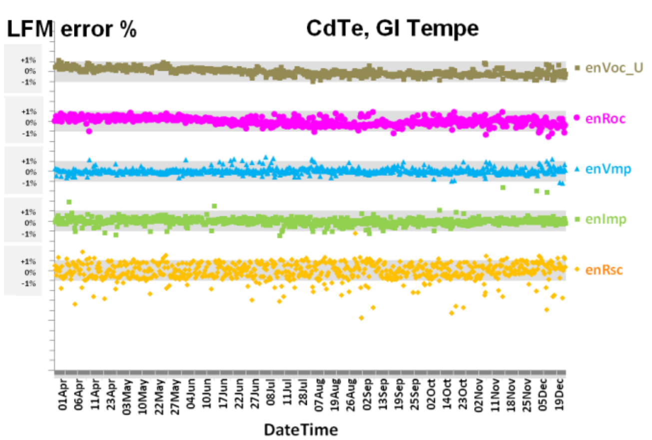

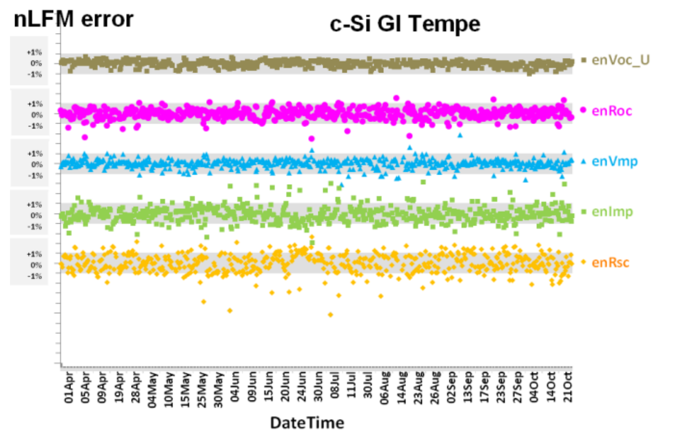

Fig 10. Prediction accuracy for 5 LFM parameters measured (dark dots) vs. calculated (light grey lines ±1%) for a CdTe (top) and c-Si(bottom) for GI Tempe.

Using some of the previously described empirical fits for spectrum, angle of incidence and module temperature the following improvements are seen

A. nIsc vs. Spectral content vs. solar altitude and azimuth

Figure 11 shows the nI_{SC} error for a CdTe module against a c-Si irradiance sensor both without (top) and with (bottom) corrections of the ISC predicted from the blue fraction. The corrected nIsc has lessened from ~10% (max in summer) to now mostly within ±2% (flat over the year) with only a small ripple around November and December when the sun is lowest and the correction needed greatest and most uncertain

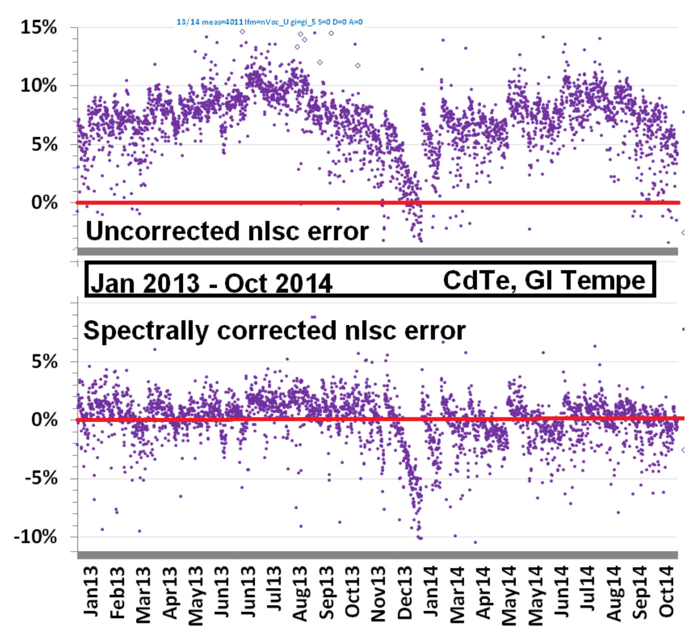

Fig 11. Improvement to modelled nI_{SC} errors from empirical spectral correction (bottom) for a CdTe module at GI Tempe

B. nI_{SC} vs. Sensor type angle of incidence

Figure 12 shows the modelled vs. measured nI_{SC} error for a cSi module against a c-Si irradiance sensor and pyranometer

(a) vs. a c-Si reference cell. Most points are within <±1% but there is a degree of scatter

(b) vs. a pyranometer uncorrected for aoi. The best errors are <±1% (when the aoi is low so corrections aren't needed), when the aoi is high the errors can be worse than -15% (see figure 8 – this loss is expected from an aoi of 75degrees)

(c) vs. a pyranometer empirically corrected for aoi. The average errors are now <±2% but this can probably be improved a little by parameter optimization.

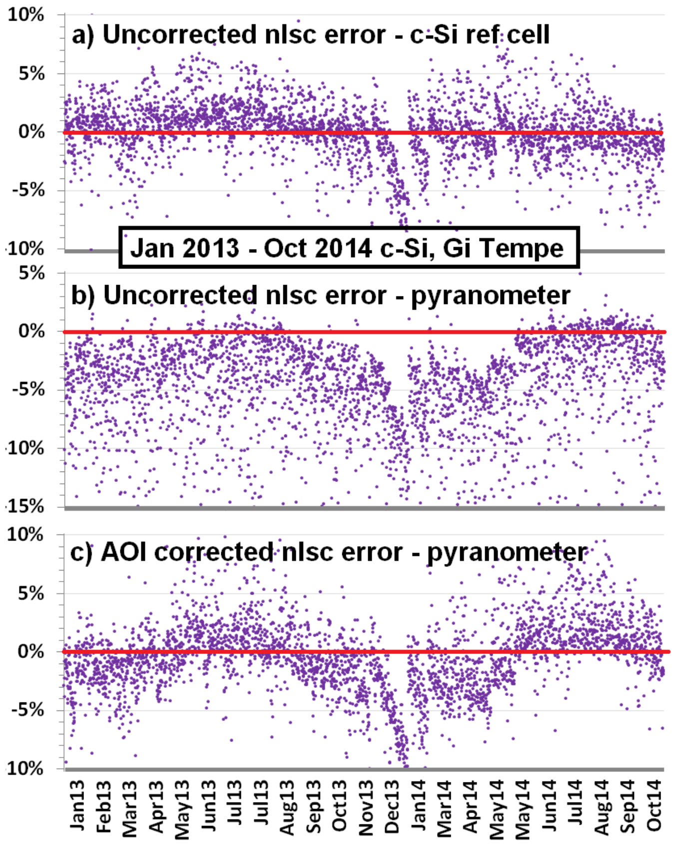

Fig 12. Improvement to modelled nI_{SC} errors from empirical angle of incidence correction for a c-Si reference cell and a pyranometer for a c-Si module at GI Tempe.

VI CONCLUSIONS

- PV_LIB is being integrated into Gantner Instruments measurement data and analysis methods [9]
- LFM is compatible in line with PV_LIB algorithms and will gain further understanding for modelling
- Efficient data filters allow more reliable data analysis and interpretation
- Standardization of algorithms, reduction of site specific impacts allows reliable plant benchmarking within the portfolio
- Empirical modelling with PV_LIB functions enhances LFM fits leading to reduced errors even without spectral information, reference cell or module temperature measurements.
- Gantner Instruments will introduce LFM and PV_LIB to its real time platform (gantner.webportal) which enables more accurate utility scale performance verification, analysis and prediction.
- This provides more accurate performance analysis, indication of abnormal loss or trends leading to more effective O&M and risk reduction for owners on a real time basis.
- Performance guarantees – target versus actual performance – can be validated more reliable as the difference can be linked to the integrated loss stages where optimization potential (in terms of kWh or $) can be identified as well.
- Sandia National Laboratories plans to incorporate the LFM model into the next release of the PV_LIB Toolbox.

ACKNOWLEDGEMENTS

Sandia National Laboratories is a multi-program laboratory managed and operated by Sandia Corporation, a wholly owned subsidiary of Lockheed Martin Corporation, for the U.S. Department of Energy's National Nuclear Security Administration under contract DE-AC04-94AL85000.

Thanks to Norbert Kleber for the database queries and help.

REFERENCES

[1] Stein, J.: The PVPMC *38th PVSC, Austin, TX 2012*

[2] Andrews, R. W., Stein, J., Hansen C. and Riley, D.: Introduction to the Open Source PV LIB for Python Photovoltaic System Modelling Package. *40th PVSC Denver, CO 2014* .https://pvpmc.sandia.gov/

[3] Holmgren, W. et al PV_LIB Python *42nd PVSC, New Orleans 2015*

[4] Ransome, S. and Sutterlueti, J.: "5BV.2.18 Using the Loss Factors Model to Improve PV Performance Modelling for Industrial Needs" *29th PVSEC Amsterdam 2014*

[5] Stein, J. et al.: "4CO.11.1 Outdoor PV Performance Evaluation of Three Different Models: Single-diode, SAPM and Loss Factor Model", *28th PVSEC, Paris, 2013*

[6] Ransome, S.: "#581 Energy Modelling and Rating - Area 9 Plenary" *40th PVSC Denver CO 2014*

[7] Reda, I. and A. Andreas (2008). Solar Position Algorithm for Solar Radiation Applications. *Golden, Colorado, National Renewable Energy Laboratory.*

[8] *IEC 61215* - NOCT section 10.5

[9] Gantner Instruments Webportal http://demo.gantner-webportal.com